The 25th Iranian Conference on Optics and Photonics (ICOP 2019), and the 11th Iranian Conference on Photonics Engineering and Technology (ICPET 2019).
University of Shiraz,
Shiraz, Iran,
Jan. 29-31, 2019

Shiraz University

اثر زاویه تابش بر روی الگوی پراش در حسگر خورشید

مرضیه افخمی[۱]، حسین فروزان[۲]، سیمین علیبانی[۳]، محمد علی اصنافی[۴] و بهروز رییسی[۵]

[۱] گروه حسگرهای فضایی، پژوهشکده مکانیک، پژوهشگاه فضایی ایران marziafkhami@gmail.com
[۲] گروه حسگرهای فضایی، پژوهشکده مکانیک، پژوهشگاه فضایی ایران h.forouzan@isrc.ac.ir
[۳] گروه حسگرهای فضایی، پژوهشکده مکانیک، پژوهشگاه فضایی ایران alibani.simin@ gmail.com
[۴] گروه حسگرهای فضایی، پژوهشکده مکانیک، پژوهشگاه فضایی ایران rossanelski2009@yahoo.com
[۵] گروه حسگرهای فضایی، پژوهشکده مکانیک، پژوهشگاه فضایی ایران b.raeisy@isrc.ac.ir

چکیده- یک طراحی اپتیکی جامع از حسگر خورشید نیازمند در نظر گرفتن اثر زاویه تابش فرودی بر روی الگوی پراش در صفحه آشکارساز است. بدین منظور الگوی پراش بر مبنای انتگرال فرنل- کیرشهوف با استفاده از متلب شبیه سازی شده است. نتایج نشان می‌دهد که با افزایش زاویه ورودی تابش خورشید، زاویه تابش خروجی جابجا و پهنای الگوی پراش نیز افزایش می‌یابد. بنابراین انتظار داریم که با افزایش زاویه، دقت حسگر کاهش یابد.

کلید واژه- پراش فرنل، حسگر خورشید.

The Effects of Angle of Incidence on Diffraction Pattern in the Sun Sensor

Marzieh Afkhami, Housein Forouzan, Simin Alibani, Mohammad Ali Asnafi

and Behrouz Raeisy

Space Sensor Group, Institute of Mechanics, Iranian Space Research Center

Abstract- The comprehensive optical design of sun sensor needs considering the effect of sunray's angle on the diffraction pattern on the detector plane. For this purpose the diffraction pattern has been simulated on the basis of Fresnel –Kirchhoff integral using MATLAB. The results indicate that by increasing the angle of incoming Sunray the peak location shifts and the diffraction width increases, consequently, the accuracy of the sensor decreases in large angles.

Keywords: Fresnel Diffraction, Sun Sensor.

1. Introduction

The Sun sensor is one of the most important parts of attitude determination and control system of satellite's missions. The function of the Sun sensor is to determine the angular position of Sun relative to a certain reference axis or plane of a Sun sensor in one or two directions [1]. The principle of the measurement of the Sun sensor is schematically shown in Fig. 1. A thin opaque layer with a narrow slit is placed above a perpendicular linear array detector. The Sun based on the diffraction pattern, illuminates different pixels in dependence on the angle to main sensor axis. To protect the detector against direct radiation, and to fit the appropriate exposure of the image sensor a special attenuation-filter is used as a front window [2, 3]. The field of view (FOV) indicates the range of Sun angles which can be measured by the Sun sensor, as shown in Fig. 1. The FOV in *x* direction can be determined by Eq. (1):

$$FOV = 2\arctan(\frac{a}{2h}) \qquad (1)$$

Where *a* is the length of the detector and *h* is the distance between slit and the detector. According to Eq. (1), the distance between the detector and the slit, *h*, defines FOV of the Sun sensor. By analysing the location of the Sun's diffraction pattern on the image detector plane, the Sun angles (α) can be calculated as:

$$\alpha = arc\tan(\frac{x_i}{h}) \qquad (2)$$

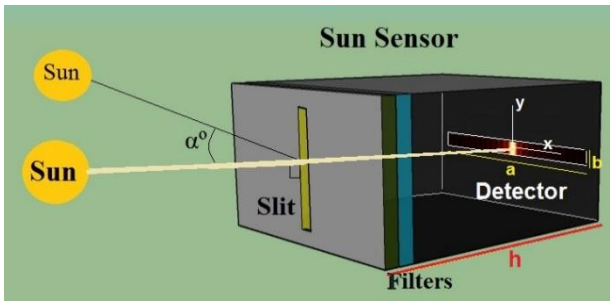

Fig. 1: Schematic of Sun sensor with image detector plane.

Where x_i denotes the coordinate of the Sun pattern's center in x direction (Fig. 1).

A single slit diffraction can be divided into Fresnel diffraction and Fraunhofer diffraction. In Fresnel diffraction, either the incident wavefronts on the slit, or the diffracted wavefronts from the slit, or both, are not planar. Because of the finite distance between the slit and the linear array detector, Fresnel diffraction approximation is appropriate to describe the diffraction in the Sun sensor.

Diffraction calculus is generally performed numerically, which involves a double integral of a complex function with a fast oscillating argument. In this case, solution is usually derived in terms of certain types of diffraction integrals known as Fresnel-Kirchhoff, or Rayleigh–Sommerfeld integrals [4, 5].

In this paper to achieve the optimized design of the Sun senor, the diffraction on the detector plane (in one direction), for the different angle of the Sun, would be analysed on the basis of Fresnel diffraction theory. We employed a simple illumination model based on Fresnel diffraction from a single-slit aperture.

2. Optical simulation of the Sun sensor

The large distance between the sensor and the Sun allows us to assume that the incident light arrives as plane waves. Based on Fresnel-Kirchhoff formula, the intensity distribution of diffraction image can be calculated through Eq. (3).

$$\tilde{E}(P) = \frac{A}{i\lambda}\iint_{slit}\frac{e^{ik\,[x_0\,\cos(\alpha)+y_0\,\cos(\beta)+r]}}{h}\,d\sigma \qquad (3)$$

Where λ is the wavelength; A is constant which indicates the electric field intensity of the incident Sun ray; k is the wave vector; h is the distance between slit and the detector; α and β denote two direction cosines of the incident Sun ray. The width of the slit has to be optimized to get the best light pattern on detector. If the slit is too shallow, there will be diffraction stripes. If it is too wide, the resolution will be decreased. So, the first work of optical designing of the Sun sensor is to determine the width of the slit. Based on the Eq. (3), the distribution of light pattern with different width slits is simulated in MATLAB [6, 7]. Light propagating through the sensor is considered to consist of a single wavelength. The wavelength chosen corresponds to the peak sensitivity of the detector array; this could be physically approximated by substituting a band-pass filter after the slit. The detector sensitivity peaks at λ=550nm, the response curve of the linear array detector using in this paper is shown in Fig. 2.

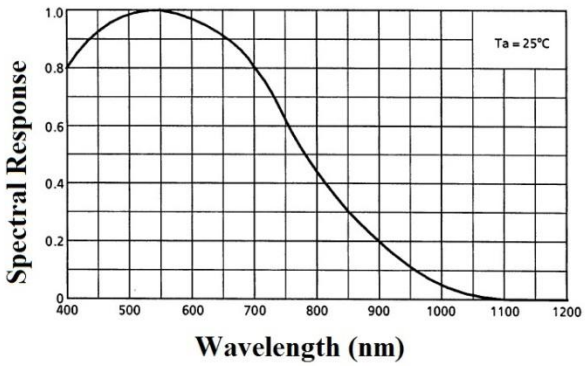

Fig. 2: Spectral response curve of the detector.

When the incident Sunray is perpendicular to the slit ($\alpha = 0^{\circ}$ and $\beta = 0^{\circ}$), Fig. 3 shows the central width of diffraction pattern that we will get on the image detector plane (1pixel = 8μm) with different aperture sizes. According to the simulation results with the increase of the aperture size, the width curve of the diffraction spot goes sharp at first indicating that the contrast of the diffraction pattern gets enhanced. However, once the maximum intensity of the diffraction pattern is reached, the simulated results also indicated that there is a reduction in contrast of the diffraction pattern with further increase of the aperture size.

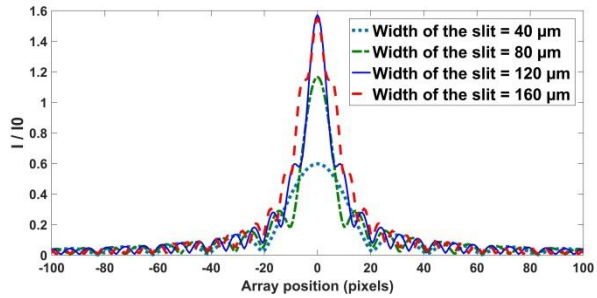

Fig. 3: The diffraction pattern with different aperture sizes at h = 8 mm.

According to the simulation results shown above, when the slit width is set as 80 μm, the light pattern is at its best state. Thereby, the width of the slit is designed to be 80 μm in the following. As shown in the Fig. 4, by setting the width of the slit at 80 μm, it can make a single peak output in the detector plane. It is expected that with having a single peak (where the side-lobes intensity are considerably less than the main-lobe intensity), the accuracy of the sensor will increase.

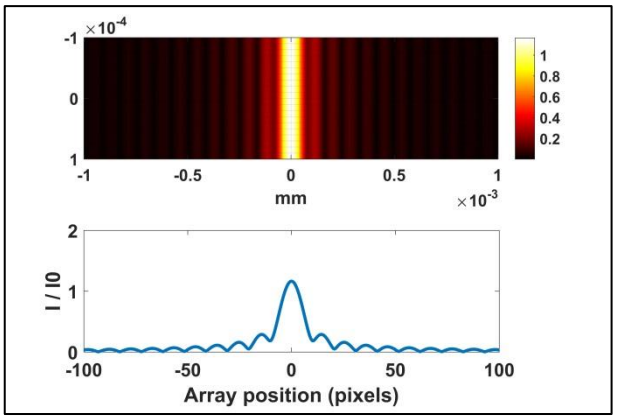

Fig. 4: The Fresnel diffraction model of Sun sensor with a slit aperture with width = 80μm on the detector plane.

The numerical simulation based on Eq. (3) can be conducted to analyse the diffraction pattern with respect to the distance between slit and detector plane, *h*. As shown in Fig. 5, when the incident Sunray is perpendicular to the slit, the diffraction patterns of 80μm width of the slit with respect to different *h* have been simulated and the light intensity has been normalized. The results indicated that with the increase of *h*, the diffraction effect is more striking and the size of diffraction pattern also increases.

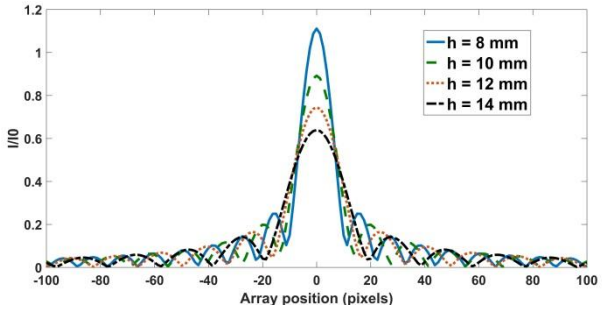

Fig. 5: The diffraction patterns of a slit with width = 80μm, with respect to different h.

2.1. The effect of incident angles

The conditions of oblique incidence are taken into account. The numerical simulation has been conducted to analyse the diffraction effect with oblique incident Sunray and the results are shown in Fig. 6. The incident Sun ray is oblique along *x* axis with different angles ($\alpha \neq 0^{\circ}$ and $\beta = 0^{\circ}$) and the slit size is fixed at 80 μm. Based on the simulation results, the diffraction pattern will stretch in the same direction (*x* axis) and if the incident Sun angle gets larger, the diffraction pattern will stretch longer along the incident direction.

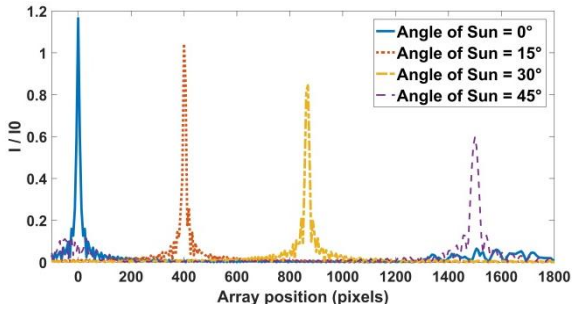

Fig. 6: The diffraction patterns with slit width = 80µm and h= 12 mm, with respect to different angle of the Sun (α) in the x direction.

As shown in Fig. 6 when angle of the Sun is α = 45°, the number of illuminated pixel (the pixel number which is required in peak detection algorithm) is up to 1500. Therefore, for FOV = 45° and h = 12 mm, it is needed a detector with more than 1600 pixels to ensure that the diffraction pattern of the Sun (place in detector) for measuring the angle of Sun in desired FOV. Furthermore the diffraction pattern with respect to different incident angles and various distances between slit and detector have been simulated. Fig. 7 demonstrates the number of illuminated pixels which will be extracted as a Sun pattern for h = 8mm.

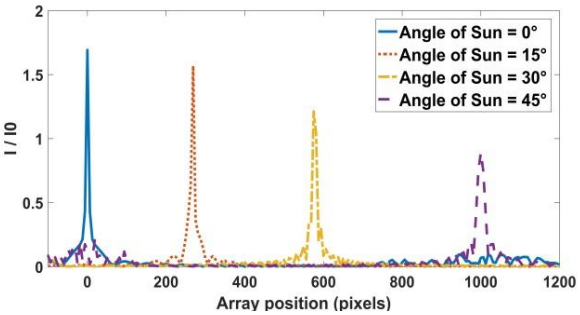

Fig. 7: The diffraction patterns with slit width = 80µm and h= 8 mm, with respect to different angle of the Sun.

For measuring the FOV = 45° with distance 8 mm between slit and detector, a linear detector array with 1200 pixels is sufficient.

3. Conclusions

Detector outputs are used to find the angle of the Sun in the Sun sensor. The output of the detector is the vector containing the light intensity of the detector pixels, which the intensity of each pixel is proportional to the position of the light beam illuminated on it.

By setting the width of the slit, it can make a single peak output in the detector. By assuming the proper slit width, the results of the analysis on the output of the detectors show that by increasing the angle of incoming beam, in other words, increasing the field of view of the sensor, the corresponding peak location moves with the highest intensity towards the non-centred pixels.

In addition, the analysis reveals that ~~with~~ increasing the angle of incidence, the beam width is increased and the peak value is reduced. On the other hand, the precision of the algorithms for measuring the angle depends on the width of the beam, the peak size, and the amount of noise in the environment. By assuming proper slit width, increasing the beam width and reducing the maximum peak size, the decreasing the accuracy of the peak detection algorithms and thus reducing the sensor accuracy and increasing the error in finding the incident beam angle will be achieved. Therefore, it can be concluded that with the increase of the sensor field of view, the accuracy of the sensor decreases.

References

1. S. Rhee, *Fine Digital Sun Sensor (FDSS) Design and Analysis for STSat-2*. in *International Conference on Control, Automation and Systems*. 2005.
2. M. Pedersen, and J.H. Hales, *Linear Two-axis MOEMS Sun sensor*, Citeseer, 2006.
3. F. Qiao-yun, P. Jia-wen, and G. Xinyang, *Micro digital Sun sensor with linear detector*, REVIEW OF SCIENTIFIC INSTRUMENTS 87, 075003, 2016.
4. M. Born and E. Wolf, *Principles of Optics: Electromagnetic Theory of Propagation, Interference And Diffraction of Light* (Cambridge University, 1999).
5. P. G. Rudolf, JJ. Tollett, M. McGowan. *Computer modeling of wave propagation with a variation of the Helmholtz–Kirchhoff relation*. Appl Opt;29:998, 1990.
6. J. Rasanen, M. Kawazoe,E. Tenjimbayashi,T. Eiju,K. Matusda. *Computer simulation of the scatter plate interferometer by scalar diffraction theory*. Appl Opt 36; 5335, 1997.
7. Z. Zheng, T. Ding, and J. Zhang, "Characteristics of aperture-array diffraction and its application," Acta Opt. Sin. **26**, 294–299, 2006.